Modified Cyclostationarity Feature Detection for Asynchronous PU Occurrence in Cognitive Radio Systems

Ashraf A. Eltholth

***Abstract*— This paper mitigates the consequences of asynchronous primary user (PU) activities within the cognitive radio user sensing time period. The effect of arrival and departure times of PU on the joint time-frequency cyclostationarity is illustrated with the 802.11a OFDM signal and applies results obtained for an adaptive threshold based cyclostationarity feature. The proposed scaling algorithm is based on the probability of effective sample size. The proposed algorithm improves the ROC performance under various PU occurrence conditions.**

***Index Terms*—Cognitive Radio, Cyclostationarity, OFDM.**

I. INTRODUCTION

Limited spectrum resources are considered as the intrinsic barrier to growing services in wireless communications. Cognitive ratio (CR) is introduced as a value added solution to the emerging software defined radio transceivers. The idea is to allow cognitive users (CU) to access the unused spectrum resources dynamically based on sensing the spectrum before transmission strategy [1].

Hence, reliable spectrum sensing techniques are highly required to guarantee uninterrupted services to the primary users on one hand, and efficient spectrum usage on the other hand. Being of that importance, spectrum sensing gained a lot of concern by researchers in the past few years. There are many survey works that explore, categorize and analyze different types of spectrum sensing techniques [2], [3] just to name a few.

Local spectrum sensing is the most widely used technique, each CU measures the primary user (PU) signal and decides wither the channel of concern is idle or busy. Cyclostationarity-feature detection is a local sensing technique that exploits the periodicity of PU signal statistics as a property of modulation formats [4]. Mostly, feature detector is able to discriminate weak signals PU signals from noise at low SNR scenarios, where both matched filtering and blind energy detection are not appropriate [5]. Cyclostationarity sensing is gaining an increasing interest due to the diffusion of OFDM based standards in communication systems, to get benefits from the cyclostationarity existence in OFDM signals [6]. Cyclostationarity based algorithms have consistent signal selectivity as the sample space size approaches infinity [7].

The diversity of CR applications led to a cognition at heterogeneous networks with different radio access technologies. This type of cognition is titled cognitive heterogeneous networks (CHN) [8]. However, in such networks, PU may appear randomly during the SU sensing period due to timing misalignment. This is also probable in heavy-traffic networks with long sensing intervals as in cyclostationarity detection, where its performance is largely dependent on sensing period length [9].

Detecting the dynamically occurring PU signal within the sensing period has been considered as a challenge in different sensing techniques where the detection performance badly affected by this dynamic nature of PU signal. In [10], analyzed the performance of energy detection in the combined situation of random Primary user arrival and departure. The problem is further analyzed in [11] that provided analytical forms for the unequal scale sampled ED performance measures and proposed an optimal threshold setting that assure minimum detection error. In [12], an adaptive weighted sensing scheme based on power function has been proposed with simultaneous transmission for dynamic PU traffic. The proposed weighting scheme showed superior performance of sensing accuracy and energy efficiency in low SNR regime. Furthermore, in [13] the trade-off between sensing and throughput for a secondary user has been investigated under random arrivals and departures of multiple primary users. For cyclostationarity-based detector, in [9], the performance deterioration of second order cyclostationarity has been investigated in case of the random arrival and departure of primary user signal. In [14], a test statistic based on the spectral auto-coherence function has been proposed to improve the sensing performance for dynamic PU environments.

This paper proposes an adaptive threshold scaling for the second order cyclostationarity feature detector. The motivation behind this proposal is that, the asynchronous activity of PU, will affect the actual presence time of PU within the CU sensing time. Consequently, the threshold has to be scaled down with respect to the probability of effective sample time.

The paper contains 6 sections, the OFDM signal cyclostationarity is demonstrated in section II. While the PU effective Sample size distribution formula is derived in section III. Section VI presents the proposed hybrid time frequency CFD along with the proposed optimum threshold. The 802.11a signal parameters in addition to simulation results are discussed in section V. Finally, conclusions are listed in the sixth section.

II. OFDM SIGNAL CYCLSTATIONARITY

There are two types of cyclostationarity feature detection in OFDM based signals. The first is cyclic prefix based cyclostationarity, that exploits cyclic autocorrelation function generated by the CP of OFDM [15]. Consequently, the

Ashraf A. Eltholth, Transmission Department, National Telecommunication Institute, Cairo, Egypt

cyclostationarity feature is dependent on the length of CP. It has been demonstrated in [6] that the cyclic frequency α of an OFDM signal belongs to the set of integer multiples of $1/N_c$ where N_c represents the total number of subcarriers constituting the OFDM symbol.

While the second is pilot based cyclostationarity detection, that is induced by preambles or repeating information symbols over multiple bursts [15].

A. Frequency Domain CFD

The signal is said to be cyclostationary if its autocorrelation is periodic, i.e., can be presented with some set of Fourier coefficients. If the autocorrelation is periodic for some delay τ, then its frequency component at some cyclic frequency α is nonzero. This component, cyclic autocorrelation, can be estimated as with N observations as [16]:

$$\hat{R}(\tau,\alpha) = \frac{1}{N}\sum_{n=0}^{N-1} x(n)x^*(n-\tau)e^{-j2\pi\alpha n} \quad (1)$$

The estimate is a single frequency component given by the DFT of $x(n)x^*(n-\tau)$ at frequency $k=\alpha$:

$$F(k) = \frac{1}{N}\sum_{n=0}^{N-1} x(n)x^*(n-\tau)e^{-j2\pi kn} \quad (2)$$

The single frequency component can be expressed as:

$$F(k) = X_\alpha - jY_\alpha$$

The test for the existence of cyclostationarity can be performed with test statistics computed in the frequency domain as:

$$T_F = \frac{X_\alpha^2\hat{E}[Y_\alpha^2] + Y_\alpha^2\hat{E}[X_\alpha^2] - 2X_\alpha Y_\alpha\hat{E}[X_\alpha Y_\alpha]}{\hat{E}[X_\alpha^2]\hat{E}[Y_\alpha^2] - (\hat{E}[X_\alpha Y_\alpha])^2} \quad (3)$$

Where X_α and Y_α vectors are the real and imaginary parts of $\hat{R}(\tau,\alpha)$ respectively, calculated from (1), and $\hat{E}[.]$ is the expectation operator.

Under the null hypothesis, the test statistic is Chi-square distributed, with two degrees of freedom [15], and consequently the decision threshold η is calculated as the inverse chi-square of (1-P_{FA}), where P_{FA} is the false alarm probability.

B. Time Domain CFD

Although the frequency domain CFD test statistic is implementable, and provide the ability to observe simultaneously multiple cyclic frequencies, it can be noted that the frequency domain conversion can be skipped. However, the required terms to calculate the test statistics are available in time domain [15].

By denoting $x_{t,\alpha}$, and $y_{t,\alpha}$ vectors as the real and imaginary parts respectively of:

$$x(n)x^*(n-\tau)e^{-j\frac{2\pi\alpha n}{N}}$$

The test statistics can be computed as:

$$T_T = \frac{X_{t,\alpha}^2\hat{E}[y_{t,\alpha}^2] + Y_{t,\alpha}^2\hat{E}[x_{t,\alpha}^2] - 2X_{t,\alpha}Y_{t,\alpha}\hat{E}[x_{t,\alpha}y_{t,\alpha}]}{\hat{E}[x_{t,\alpha}^2]\hat{E}[y_{t,\alpha}^2] - (\hat{E}[x_{t,\alpha}y_{t,\alpha}])^2} \quad (4)$$

Where $X_{t,\alpha}$ and $Y_{t,\alpha}$ can also be computed directly from the real and imaginary parts of (1) without the FFT, at the predetermined (t, α), While $\hat{E}[.]$ is the expectation operator of the corresponding vector for the predetermined α.

III. PU Effective Sample Size Distribution

In tele-traffic theory, the customers' arrivals are supposed to follow Poisson distribution, especially when a large number of independent users are served. The probability that PU will arrive after time q is given by [17]:

$$P(T) = e^{-\lambda_a T} \quad (5)$$

Where λ_a is the mean arrival rate. Being a discrete random variable, the time $= nT_s$, where T_s is the sampling time, for simplicity, T_s will be assumed to be 1. Hence the probability of arriving PU at the n_0 sample within the sensing period is given by [10]:

$$P(n_0) = e^{-n_0\lambda_a} - e^{-(n_0+1)\lambda_a} \quad (6)$$

While the probability mass function of PU departure at n_1 sample given that it arrived at n_0 is given by:

$$P(n_1|n_0) = e^{-n_0\lambda_d}(e^{-n_1\lambda_d} - e^{-(n_1+1)\lambda_d}) \quad (7)$$

Where λ_d is the mean departure rate.

The PU sample size assuming that it arrives and departs within the sensing time is illustrated in Fig. (1)

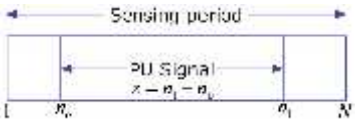

Figure 1. PU sample size

$$P(z) = \sum_{n_0=1}^{N} P(n_0, n_1 - z - n_0) \quad (8)$$

Not to mention that the arrival and departure are independent random processes, thus:

$$P(z) = \sum_{n_0=1}^{N} P(n_0)P(n_1|n_0) \quad (9)$$

Substituting equations (6) and (7) in (9):

$$P(z) = \sum_{n_0=1}^{N} e^{-n_0\lambda_a} - e^{-(n_0+1)\lambda_a} \times e^{n_0\lambda_a}(e^{-n_1\lambda_d} - e^{-(n_1+1)\lambda_d}) \quad (10)$$

$$P(z) = \sum_{n_0=1}^{N} e^{-n_0\lambda_a}(1 - e^{-\lambda_a}) \times e^{n_0\lambda_a}e^{-n_1\lambda_d}(1 - e^{-\lambda_d}) \quad (11)$$

Substituting $n_1 = n_0 + z$ in equation (11) we get:

$$P(z) = e^{-z\lambda_d}(1 - e^{-\lambda_a})(1 - e^{-\lambda_d})\sum_{n_0=1}^{N} e^{-n_0\lambda_a} \quad (12)$$

The sum of trigonometric series part is given by:

$$\sum_{n_0=1}^{N} e^{-n_0\lambda_n} = e^{-\lambda_n}\left(\frac{(1-e^{-\lambda_n N})}{(1-e^{-\lambda_n})}\right) \quad (13)$$

From equations (12) and (13), the probability mass function of the PU sample size existing within the sensing period is given by:

$$P(z) = e^{-\lambda_n} e^{-z\lambda_d}(1-e^{-\lambda_n N})(1-e^{-\lambda_d}) \quad (14)$$

IV. PROPOSED MODEL

This Paper proposes the use of hybrid Time-Frequency CFD that computes the test statistics in the two domains then selects the largest of them. The motivation behind this proposal is that the test statistics calculation formulas are the same on different terms as depicted in (3) and (4)

The decision threshold has to be modified to reflect the effect of random activities of PU within the sensing time. That is calculated as the inverse Chi-square with two degrees of freedom on the joint probability of PU existence in the sensing time $(1-P_{FA})$ and the effective PU sample size within the sensing period derived in (14):

$$\eta = F^{-1}_{\chi^2_2}(1-P(z)).(1-P_{FA}) \quad (15)$$

V. SIMULATION & DISCUSSIONS

The CFD algorithm described in section IV is applied on an IEEE 802.11a signal format. The 802.11a operates in the 5 GHz band, and uses a 52-subcarrier OFDM with a maximum data rate of 54 Mbit/s.

A. 802.11a OFDM Signal

IEEE 802.11a signal is a pulsed type signal with parameters as depicted in table I.

The OFDM symbol is composed of 52 subcarriers; with 48 data subcarriers plus 4 pilot sub-carriers. The mentioned modulation formats in table I can selected to provide different data rates. It can be noted that the guard interval is one fourth of the data interval, and the total number of samples in the regular OFDM symbol is 80.

Table I

802.11a OFDM Physical Parameters

Parameter	Value
Bandwidth	20 MHz
Total subcarriers	52
Data subcarriers	48
Pilot subcarriers	4
Sub-carrier Frequency Spacing	312.5 KHz (20MHz/64)
Information Rate	6/9/ ... / 54 Mbps
Modulation	PSK, QPSK, ... 64 QAM
Coding Rate	1/2, 2/3, 3/4
FFT sample size	64 point
OFDM Symbol size	80 point (64 + 16)

The frame structure of the 802.11a signal burst is depicted in Fig. 2:

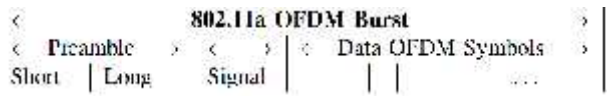

Figure 2. 802.11a Frame Structure

The burst starts with a preamble for channel equalization in addition to synchronization purposes. The burst length and other selected physical parameters information are sent in the SIGNAL field using BPSK. Multiple data OFDM symbols are appended in the burst.

B. Simulation Results

The above mentioned 802.11a signal is simulated with Matlab R2014a, according to the following details:

* The short preamble consists of 10 short OFDM symbols each of 16 subcarriers; it is used for channel equalization. While the long preamble consists of two regular size OFDM symbols each of 64 subcarriers plus GI 16 subcarriers, it is used for channel estimation and frequency offset detection.

* The SIGNAL field consists of a regular OFDM symbol, containing information about the signal physical parameters.

* The simulated signal burst contains 19 OFDM data symbols, meaning that, the total number of samples is 1920 in each burst. The burst duration in 96 µs, this means that the signal bandwidth is 20 MHz as shown in Fig. 3:

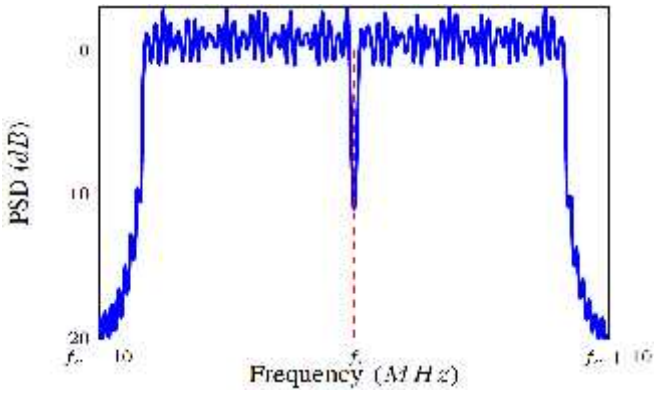

Figure 3. 802.11a Signal Spectrum

It can be noted that, the signal occupies 20 MHz total bandwidth, with a null sub-carrier at the center.

Based on simulation results shown in figures 4 and 5, it can be noticed that the CAF magnitude of the 802.11a signal has the following properties:

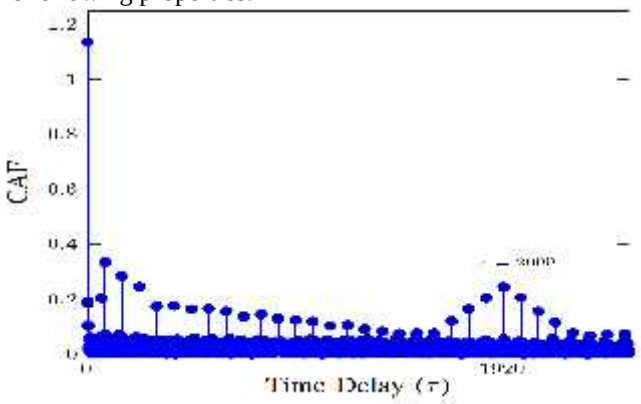

Figure 4. Time Domain CAF

It has significant values at multiple integer delays of 1920 at zero cyclic frequency, due to the presence of preamble symbols as depicted in Fig. (4). Furthermore, around each of the above mentioned locations, there exist other nonzero values of the CAF at delays of multiple integers of 80 due to the existence of guard intervals in the OFDM symbols inside the signal burst.

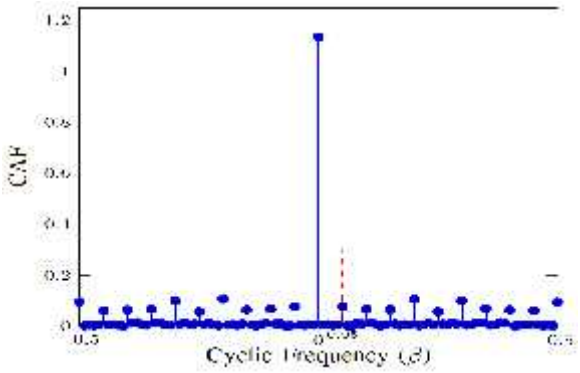

Figure 5. Frequency Domain CAF

It is significant values in the frequency domain at cyclic frequencies equal to integer multiples of ±0.05 as illustrated in Fig. (5).

When applying the CFD algorithm on the 802.11a simulated signal, the ROC curve is depicted in figures 6 and 7:

It can be noted from Fig. (6) that the ROC of the CFD is severely affected by the PU random activities within the sensing period. Moreover, the performance degradation is nearly independent on the specific arrival or departure rates, as illustrated by the wrapped curves around each other corresponding to different arrival and departure rate values.

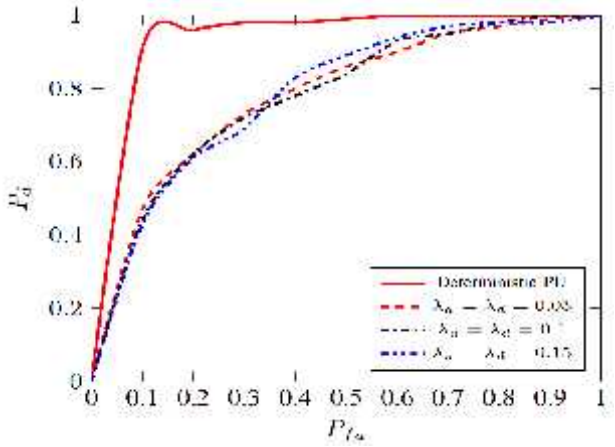

Figure 6. ROC of the CFD at SNR = -15 dB

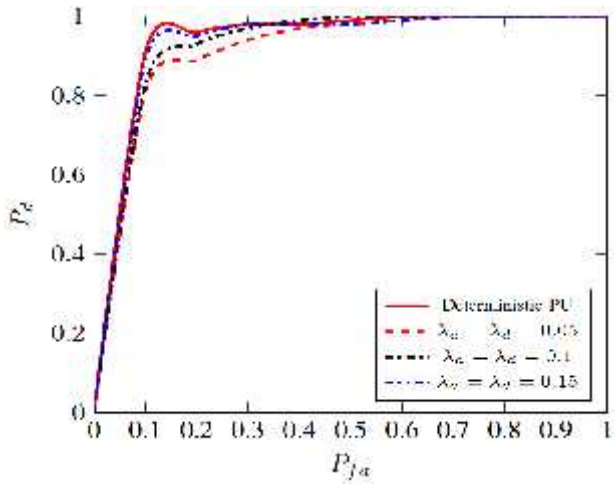

Figure 7. ROC of the Modified CFD at SNR = -15 dB

The modified CFD algorithm proposed in this paper greatly mitigate the effect of PU random activities in the CU sensing period as depicted in figure 7, as the ROC curves appear in the vicinity of the deterministic situation when no random activities situation is assumed.

For the sake of numerical evaluation of the proposed algorithm performance, the area under the curve values for above mentioned situations in figures 6 and 7 are listed in table II:

Table II
Area Under the Curve Measurements

$\lambda_a = \lambda_d$	Area Under the Curve %		% of the deterministic situation	
	CFD	Modified CFD	CFD	Modified CFD
0.05	77	90.6	82.8	97.4
0.1	76.9	92	82.7	98.9
0.15	77.4	92.8	83.2	99.8

Confirming the results derived from the figure 6, the area under the curve values are far lower (about 83 %) of the deterministic situation. Moreover, different rates $(\lambda_a = \lambda_d)$ cause nearly the same value of the area under the curve.

The Modified CFD results also show a full agreement to that depicted in figure 7, as the performance enhancement reaches above 97% of the area under the curve value for the deterministic situation. The performance enhancement is directly proportional to the values of arrival and departure rates as the area under the curve reaches nearly the same value as that of the deterministic situation.

VI. Conclusion

The Cyclostationarity feature of the 802.11a signal can be detected due to the the cyclic prefix property of the regular OFDM symbols, and the preambles at the beginning of the signal burst. Moreover, it is easier to detect the cyclostationarity feature based on the cyclic prefix rather than the preambles.

The Asynchronous PU activities within the CU sensing time, severely degrades the CFD performance. That performance degradation cab be mitigated by adapting the appropriate threshold according to the probability of PU sample size within the CU sensing period.

The performance degradation is nearly independent on the specific arrival or departure rates, as illustrated by the wrapped curves around each other corresponding to different arrival and departure rate values.

The modified CFD algorithm proposed in this paper greatly mitigate the effect of PU random activities in the CU sensing period, as the ROC curves appear in the vicinity of the deterministic situation when no random activities situation is assumed.

The performance enhancement due to the modified CFD is directly proportional to the values of arrival and departure rates as the area under the curve reaches nearly the same value as that of the deterministic situation at $\lambda = 0.15$.

References

[1] S. Haykin, "Fundamental Issues in Cognitive Radio," in *Cognitive Wireless Communication Networks*, E. Hossain and V. Bhargava, Eds., ed Boston, MA: Springer US, 2007, pp. 1-43.

[2] E. Axell, G. Leus, E. G. Larsson, and H. V. Poor, "Spectrum Sensing for Cognitive Radio : State-of-the-Art and Recent Advances," *IEEE Signal Processing Magazine*, vol. 29, pp. 101-116, 2012.

[3] F. Khan and K. Nakagawa, "Comparative study of spectrum sensing techniques in cognitive radio networks," in *2013 World Congress on Computer and Information Technology (WCCIT)*, 2013, pp. 1-8.

[4] W. Z. S. L. Guodong Zhao, *Advanced Sensing Techniques for Cognitive Radio, in Springer Briefs in Electrical and Computer Engineering*. AG Switzerland: Springer International Publishing, 2017.

[5] L. Lu, X. Zhou, U. Onunkwo, and G. Y. Li, "Ten years of research in spectrum sensing and sharing in cognitive radio," *EURASIP Journal on Wireless Communications and Networking*, vol. 2012, 2012.
[6] D. Allan, L. Crockett, S. Weiss, K. Stuart, and R. W. Stewart, "FPGA implementation of a cyclostationary detector for OFDM signals," in *2016 24th European Signal Processing Conference (EUSIPCO)*, 2016, pp. 647-651.
[7] A. Napolitano, "Cyclostationarity: New trends and applications," *Signal Processing*, vol. 120, pp. 385-408, 2016.
[8] S. Shi, N. Liang, and X. Gu, "Resource allocation in cognitive heterogeneous networks considering the arrival of primary users," in *2015 IEEE International Conference on Communication Software and Networks (ICCSN)*, 2015, pp. 444-448.
[9] I. Atef, A. Eltholth, and M. S. El-Soudani, "Energy vs. Cyclostationarity-based Detection of Random Arrival and Departure of LTE SC-FDMA Signals for Cognitive Radio Systems," *Frequenz*, vol. 70, 2016.
[10] J. Y. Wu, P. H. Huang, T. Y. Wang, and V. W. S. Wong, "Energy detection based spectrum sensing with random arrival and departure of primary user?s signal," in *2013 IEEE Globecom Workshops (GC Wkshps)*, 2013, pp. 380-384.
[11] I. Atef, A. Eltholth, A. S. Ibrahim, and M. S. El-Soudani, "Energy detection of random arrival and departure of primary user signals in Cognitive Radio systems," in *IEEE EUROCON 2015 - International Conference on Computer as a Tool (EUROCON)*, 2015, pp. 1-6.
[12] M. Deng, B.-J. Hu, and X. Li, "Adaptive Weighted Sensing with Simultaneous Transmission for Dynamic Primary User Traffic," *IEEE Transactions on Communications*, pp. 1-1, 2017.
[13] H. Pradhan, S. S. Kalamkar, and A. Banerjee, "Sensing-Throughput Tradeoff in Cognitive Radio With Random Arrivals and Departures of Multiple Primary Users," *IEEE Communications Letters*, vol. 19, pp. 415-418, 2015.
[14] Y. Lee, S. R. Lee, S. Yoo, H. Liu, and S. Yoon, "Cyclostationarity-Based Detection of Randomly Arriving or Departing Signals," *Journal of Applied Research and Technology*, vol. 12, pp. 1083-1091, 2014.
[15] G. Gonz, R. Wichman, and S. Werner, "A study of OFDM signal detection using cyclostationarity," in *XIII Workshop on Information Processing and Control (RPIC)*, Rosario, Argentina, 2009.
[16] M. Kosunen, V. Turunen, and K. Kokkinen, "Survey and Analysis of Cyclostationary Signal Detector Implementations on FPGA," *IEEE JOURNAL ON EMERGING AND SELECTED TOPICS IN CIRCUITS AND SYSTEMS*, vol. 3, pp. 541-551, 2013.
[17] N. C. Beaulieu and Y. Chen, "Improved Energy Detectors for Cognitive Radios With Randomly Arriving or Departing Primary Users," *IEEE Signal Processing Letters*, vol. 17, pp. 867-870, 2010.

Ashraf A. Eltholth was born in Dakahlia, Egypt. He received the B. E. degree in electrical communications engineering from Menoufia University, Menouf, Egypt, in 1997. He received the M.Sc. and PhD degrees from Mansoura University in 2002, and 2009 respectively. His research interest is in cognitive radio enabling technologies, and efficient cellular network backhauling. He is currently working at the National Telecommunication Institute in Cairo, Egypt.